

Drag Reduction and Velocity Distribution in Developing Pipe Flow

Kikkeri L. V. Ramu*

Division of Water Resources, Denver, Colo.

and

J. Paul Tullis†

Colorado State University, Fort Collins, Colo.

Drag reduction and mean velocity measurements obtained for polymer injection into a developing axisymmetric boundary layer in the inlet region of a pipe are reported. Experiments were conducted in a 12-in. diam commercial steel pipe. Concentrated solutions of Polyox WSR 301 were injected into the pipe at 3.5 diam from the pipe entrance. Injection concentrations varied from 100 ppm to 2400 ppm with Reynolds number varying from 2.8×10^5 to 3.0×10^6 . Data for the inlet and fully developed regions of this study indicate that high drag reductions can be obtained in the inlet region. Drag reduction was found to depend on polymer flow rate, wall shear stress, and distance, but not to depend significantly on injection velocity or injection concentration. A four-layer mean velocity model is shown to describe the velocity profile in the developing polymeric region. The polymer interactive layer is dependent on flow and polymer characteristics. The upward shift of the turbulent layer is directly related to the dimensionless drag reduction parameter $(V/u)(\nu_p/\nu_w)$. The velocity profile in the outer flow of the developing region is described by a velocity defect law with a constant profile parameter.

Nomenclature

B	= intercept term of Newtonian semilog velocity profile	y_p^+	= value of y^+ at edge of viscous sublayer
B_p	= intercept term of log-linear velocity profile for polymer interactive layer	y_p^+	= value of y^+ at edge of polymer interactive layer
ΔB	= vertical shift of long-linear velocity profile for drag reduction flow from Newtonian flow velocity profile	$(y/\delta)p$	= value of y/δ at edge of polymeric interactive layer
C	= concentration of polymer sample	δ	= boundary-layer thickness
C_i	= concentration of injected polymer solution	η	= intrinsic viscosity
C_w	= concentration of polymer solution at pipe wall	κ	= Newtonian mixing length coefficient
C_∞	= concentration of homogeneously mixed polymer	κ_p	= mixing length coefficient for polymer interactive layer
D	= diameter of pipe	λ	= coefficient used in Eq. (7)
f_p	= friction factor for polymer flow	ν_p	= kinematic viscosity of polymer solution
f_w	= friction factor for water flow	ν_w	= kinematic viscosity of water
gm/dl	= grams per deciliter	π	= profile parameter in Eq. (8)
gpm	= gallons per minute	ρ	= mass density of liquid
k_s	= equivalent sand grain roughness	τ_w	= shear stress at wall
k^+	= $k_s u^* / \nu_w$		
M_w	= average molecular weight		
ppm	= parts of polymer per million by weight		
Q_i	= injection rate of polymer solution		
Re	= flow Reynolds number = VD/ν_w		
U_c	= mean core velocity		
u	= local mean velocity in x-direction		
u^*	= shear velocity = $\sqrt{\tau_w/\rho}$		
u^+	= u/u^*		
V	= bulk mean velocity in pipe		
x	= coordinate in flow direction measured from pipe entrance		
y	= coordinate in radial direction measured from pipe wall		
y^+	= yu^* / ν_w		

Introduction

THE high drag reduction obtained in turbulent shear flows containing small amounts of high molecular weight polymer is well-documented. Various types of polymers have been used in drag reduction studies either in fully developed pipe flows or boundary-layer flows over flat plates. Several attempts have been made to explain the mechanism of drag reduction.¹ However, a theory which explains the interaction between polymer macromolecules and the turbulent shear flow is not yet available. To get an insight into the gross features of the flow, investigators have relied on the phenomenological theories and experimental data to come up with parametric dependence of both drag reduction and mean velocity profiles, on the polymer characteristics, its concentration, and certain flow parameters.

Application of drag reduction techniques to submerged bodies would require injecting concentrated polymer solutions at the boundary. Investigations have shown that drag reduction is primarily a function of the polymer content near the wall. Therefore, when a polymer solution is injected at the boundary, the reduction in wall shear stress should be greater than that for the same amount of polymer homogeneously mixed with the flow. The wall concentration will depend on the polymer diffusion characteristics.

Results of a drag reduction investigation carried out by injecting a concentrated polymer solution into a developing axisymmetric boundary layer formed in the inlet reach of a 12-in. diam commercial pipe are presented. The synthetic

Received June 3, 1974; revision received May 29, 1975. This program was carried out with support from the National Science Foundation, Grant No. GK-25339, and support from the Naval Ship Systems Command, General Hydromechanics Research Program, Contract N00014-67-A 0299-0013. Appreciation is expressed to these two organizations for their financial assistance.

Index category: Hydrodynamics.

*Water Resources Engineer.

†Associate Professor of Civil Engineering.

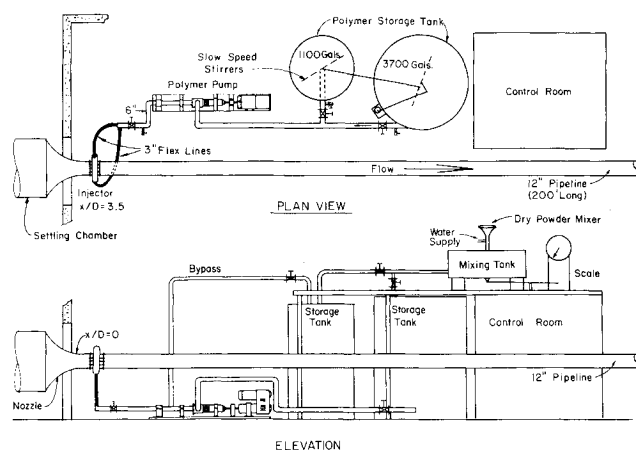


Fig. 1 General layout of test facility.

polymer used in this study was Polyox WSR 301, a poly (ethylene oxide) polymer manufactured by Union Carbide Co. It is a linear polymer having an average molecular weight of about 4×10^6 . The viscosity characteristic of the polymer solution was also studied.

Based on Newtonian similarity laws, a four-layer mean velocity model is presented which, from experimental results, is shown to be valid for the developing polymeric field of the inlet region. This model is compared with other mean velocity models, which have been proposed essentially for homogeneous dilute polymer flows, in fully developed pipe flows.

Experimental Facility and Procedure

The investigation was carried out in a 12-in. diam commercial steel pipe 200 ft long, with a roughness value k_s/D of 0.00038 (see Fig. 1). A settling chamber and nozzle were provided to suppress turbulence and create a uniform velocity at the entrance. The magnitude of turbulence intensity in the core flow, referred to the bulk mean velocity, was of the order of 3 to 3.5%.² The converging nozzle of the settling chamber was calibrated and used to measure the water flow. The Reynolds number in the test varied from 2.8×10^5 to about 3×10^6 , corresponding to bulk mean velocities ranging from 4.2 to 45 fps.

Concentrated solutions of polymer were mixed in a 500-gal mixing tank equipped with a dry powder aspirator, using untreated reservoir water. The mixed solution was stored in holding tanks equipped with a paddle mixer, which gently stirred the solution. Normally, polymer solutions were mixed 24 hr before a test run and agitated for 2 hr during mixing and an hour before a test run to obtain a uniform mix. For runs where concentration profiles were obtained, rhodamine WT dye was added to polymer solution in the holding tanks. The polymer concentration varied from 100 to 2400 ppm while the dye concentration was always kept at 1 ppm.

The polymer was injected into the test pipeline using a variable-speed auger-type pump. The auger-type pump and large-diameter suction and delivery lines permitted the polymer solution to be handled with negligible shear degradation. Polymer flow rate was computed volumetrically by timing the drop of the liquid level in the holding tanks. A perforated pipe section was used as an injector in this study. The injector had 4 circumferential rows of 48 holes per row. The holes were 0.375 in. in diam, and were drilled at 30° to the pipe axis. The centerline of the injector was located 3.5 diam downstream from the pipe inlet. The injection rate varied from 20 to 160 gpm, with the injection velocity normally kept below 1/15th of the bulk mean velocity, to minimize injection disturbances. The far downstream fully mixed concentration (C_∞), generally varied from 1 to 24 ppm, while some drag reduction data were obtained for C_∞ as high as 76 ppm.

Drag reduction in the inlet region and the downstream fully developed region was calculated from friction values obtained by pressure drop measurements along the pipe. For this, piezometer rings were placed every two to eight pipe diameters in the inlet reach and at longer intervals downstream. The pressure drops were measured with differential pressure transducers. Checks were made with inclined manometers, especially when the pressure drop was less than 0.1 psi.

The procedure for obtaining drag reduction was first to measure the pressure drop and calculate the friction factor for each section of pipe over the range of Reynolds numbers without polymer injection. It was confirmed that injecting water did not alter the water friction factor. Concentrated polymer solution was then injected, the pressure drop measured, and the friction factor calculated for the same section of the pipe. The percent drag reduction was computed from the following equation

$$\text{Drag reduction} = 100(f_w - f_p)/f_w \quad (1)$$

in which f_w is the measured friction factor for a given section of pipe for water flow and f_p is the friction factor at the same location in the pipe for the same Reynolds number with polymer injection.

Mean velocity was measured using specially built pitot rakes. The pitot rake consisted of 8 total head tubes mounted on an airfoil section. The stainless steel total head tubes were of two sizes. Three tubes closest to the wall were 1/32-in. i.d. with 1/16-in. o.d., while the remaining five tubes were 1/16-in. i.d. and 1/8-in. o.d. The pitot rake with its traversing mechanism was mounted in a 2-ft long 12-in. diam pipe, which could be installed at various locations along the pipe. The distance of the tubes from the pipe wall was read from an attached caliper-dial gage to the nearest 0.001 in. Normally, 30 mean velocity readings were obtained over the 6-in. radius of the pipe. The pitot rakes were calibrated in the test pipeline.

Polymer concentration samples were obtained at 12 different locations on the radius of the pipe, using the above pitot rake. For this, the samples were withdrawn through the pitot tubes immediately following a velocity measurement, without changing the flow and polymer injection conditions. The wall concentration sample was withdrawn from a wall piezometer. The dye concentration of each sample was determined with a fluorometer. The polymer concentration of the sample was obtained by relating the dye content of the sample to the polymer concentration and dye content of the injected polymer. It was assumed, based on the work of Wetzel et al.,³ that the polymer and dye diffuse together.

Characterization of the polymer solution was limited to the basic evaluation of its viscosity. Viscosity of laboratory samples at various concentrations, polymer solution samples from the holding tanks, and samples withdrawn from the wall tap was measured in the laboratory using the capillary-gravity-flow-type Ubbelohde viscometer. Two different types of viscometers were used, depending on polymer solution concentration. Viscosity measurements were carried out at a temperature of 77°F.

Experimental Results

Polymer Characterization

Polyox WSR 301 is a linear polymer having an average molecular weight of about 4×10^6 . The variation of viscosity with polymer concentration is shown in Fig. 2, and can be expressed as

$$\nu_p = \nu_w [1 + (\eta C) + 0.3(\eta C)^2] \quad (2)$$

in which ν_p and ν_w are the viscosities of the polymer solution and water, respectively, η is the intrinsic viscosity (dl/g), and C is the polymer concentration (g/dl). Though viscosity is sensitive to temperature, the ratio ν_p/ν_w for a given concentration remains unaltered with temperature change, as in-

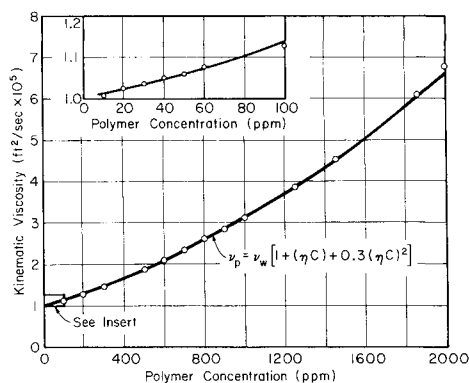


Fig. 2 Kinematic viscosity of Polyox WSR 301 at 77°F.

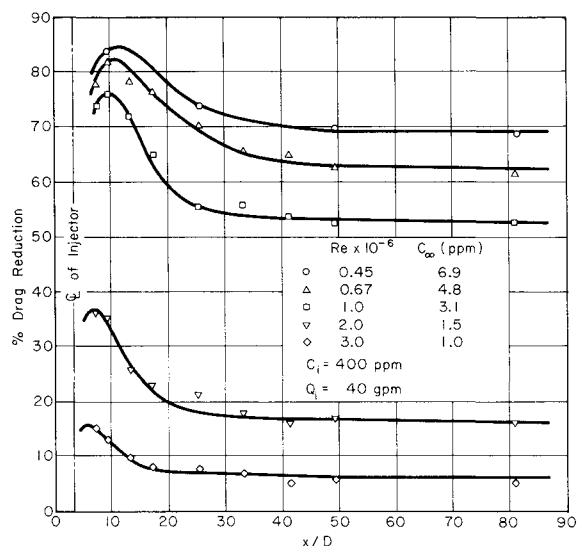


Fig. 3 Effect of Re and C_∞ on drag reduction in inlet region.

dictated by Van Driest.⁴ The intrinsic viscosity η for this polymer obtained from viscosity data was found to be 14.6 dl/g. Knowing η , the average molecular weight M_w can be determined using a power law equation⁵

$$\eta = 1.03 \times 10^{-4} (M_w)^{0.78} \quad (3)$$

With $\eta = 14.6$ dl/g, the average molecular weight of the polymer used in this study is 4.02×10^6 , compared with 4×10^6 indicated by the supplier.

Tests were carried out to determine the aging effect on polymer. For this, a stock polymer solution was prepared and its viscosity was determined at intervals of 24 hr for 10 days. After 8 days the viscosity decreased by about 2%, beyond which aging seemed to accelerate. In all the tests for this study, polymer solution was never allowed to sit for more than three days.

Drag Reduction in Inlet Region

The variation of local drag reduction with distance for one set of tests is shown in Fig. 3. Drag reduction for the first 80 diameters of the inlet was measured over lengths of 2 ft near the injector and at 4 ft and 8 ft intervals farther away. Data points shown are an average of many runs obtained by measuring pressure drop over the above lengths, and are plotted at the midpoints of these lengths. For the highest C_∞ value of 9 ppm, over 90% local drag reduction was observed. This magnitude of drag reduction was found for numerous tests covering a wide range of flow and polymer parameters. The measured values of drag reduction in the inlet region often exceeded the maximum local drag reduction measured for the

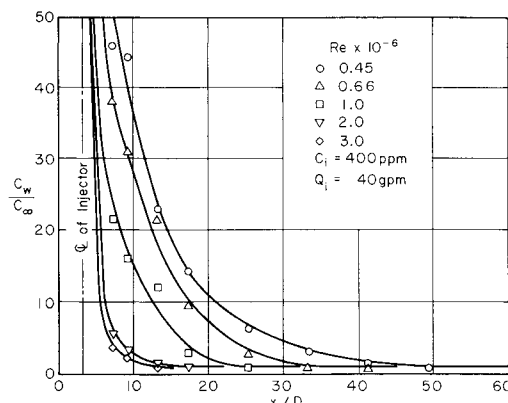


Fig. 4 Concentration profiles.

downstream fully mixed flow, which was 80% for a $C_\infty \approx 25$ ppm.

Figure 3 shows the effect of Reynolds number and C_∞ on drag reduction in the inlet region. The polymer mass flow rate for all these runs is 60.56 g/sec. The figure shows a point of maximum drag reduction, and beyond the curve rapidly drops off to a constant value. The x/D location at which the curve levels off was found to vary more with Re than with polymer mass-flow rate. The location at which the curve levels off was generally consistent with the location where the polymer became uniformly distributed across the pipe. This can be seen from Fig. 4, where the variation of wall concentration with x/D and Re is shown. At $Re = 10^6$, a uniform concentration profile exists at $x/D = 25$, which is close to the location in Fig. 3 where the drag reduction curves tend to become constant. With increasing Re , the length required for polymer to become homogeneously dispersed decreases, as seen in Fig. 4. Additional data on drag reduction, diffusion, and details regarding the injector are given in Refs. 6 and 7.

The dependence of local and total drag reduction in the inlet region on the concentration of the injected polymer was also studied. Injected polymer ranged in concentration from 100 to 2400 ppm. With higher C_i for a given Reynolds number, the point of maximum local drag reduction in the inlet region occurred farther from the injector. This is most likely a result of saturation, as the wall concentration for high C_i was above the saturation limit for longer distances from the injector. However, the total drag reduction, integrated from $x/D = 0$ to $x/D = 81$, neglecting the injector loss, was unaffected by C_i or Q_i as long as C_∞ and R were unchanged. The total drag reduction in the inlet region was greater than that for homogeneous flow, as was also observed by Poreh et al.⁸

Drag Reduction in Fully Developed Flow Region

Extensive studies on drag reduction in fully developed pipe flows with homogeneous polymer solution have been reported.¹ In the present study, drag reduction data obtained for $x/D > 100$ are shown in Fig. 5. Maximum drag reduction at all concentrations occurs in the Re range of 7 to 9×10^5 , and increases with increasing C_∞ . Drag reduction tests carried out at $Re \approx 7 \times 10^5$ over a C_∞ range from 1 to 76 ppm indicated that a maximum drag reduction of about 80% was obtained at $C_\infty \approx 25$ ppm, indicating that the curve for $C_\infty = 24$ ppm in Fig. 5 should be the enveloping drag reduction curve for this system.

Degradation

The dependence of drag reduction on wall shear stress, velocity, or Reynolds number has been well documented. Beyond the onset point, the polymer becomes more effective as the flow velocity increases. This continues up to a maximum drag reduction value for a given concentration, beyond which the drag reduction decreases, due to suspected mechanical degradation. The effectiveness of polymer is

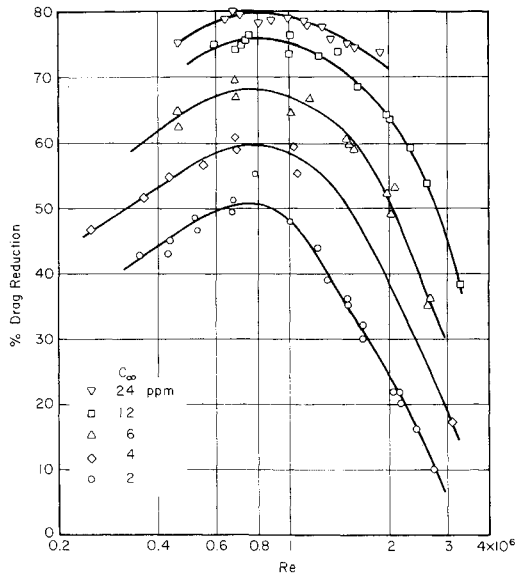


Fig. 5 Variation of drag reduction with Re and C_∞ in fully developed flow region.

related to its molecular weight, which is a measure of the length of polymer chain. When the polymer solution is subjected to sufficient shear stress the chain breaks, thus reducing its molecular weight and its drag reducing effectiveness.

Degradation in the 12-in. commercial pipe used in this study is demonstrated in Fig. 5. The pipe operated in the transition roughness regime for water flow for $3 \times 10^5 < Re < 3 \times 10^6$. Virk⁹ in his experiments found that polymer flows in rough pipes with $k^+ < 50$ where $k^+ = k_s u_*' / \nu_w$ are in an "effectively smooth" regime. In the present study it was estimated that the k^+ values exceeded this limit only for $Re = 3 \times 10^6$ and $C_\infty = 2$ ppm. Thus, only at high Re and low C_∞ will the pipe roughness influence the drag reduction. It is, therefore, concluded that for in both the inlet region and the fully developed flow region for $Re > 7 \times 10^5$ the decrease in drag reduction is due mainly to degradation of polymer and not a roughness effect. The higher concentrations are less susceptible to degradation, as seen in Fig. 5, because, at a given shear stress, the proportion of polymer chains being broken is less at higher concentrations.

Mean Velocity Models in Polymer Flows

Considerable effort has gone into formulating a suitable similarity law correlation for drag-reducing flows. These studies have been for the dilute homogeneous polymeric field in either fully developed pipe flows or flat-plate boundary layer, with a smooth boundary. The basic lack of a theory to explain the interaction between the polymer molecules and the turbulence field in a shear flow has resulted in extending the Newtonian similarity laws to polymer flows with modifications, based on friction and mean velocity data.

Over the past two decades several mean velocity models have been suggested.¹ One class of model termed the "thickened sublayer model," proposed by Meyer, considers the shear layer to consist of a thickened sublayer and a turbulent layer. He concluded that the Newtonian viscous sublayer increased in thickness with drag reduction due to damping of the local velocity fluctuations. Virk,¹¹ Van Driest⁴, Tomita,¹² among others, have proposed a three-layer model. Called the "interactive layer model," they consist of a sublayer, which is similar to the Newtonian viscous sublayer, an interactive layer, and a turbulent layer. The polymer turbulence interaction, however it might occur, is considered confined to the buffer region defined for nondrag reducing flows, which is called the "interactive layer." The velocity profile in this layer is indicated to be part of an asymptotic log-linear profile under maximum drag reduction condition.

From friction and velocity experiments mostly carried out in small diameter pipes, this asymptotic profile has been given as

$$\text{Giles}^{13} \quad u^+ = 5.35 (y^+)^{0.396} \quad (4a)$$

$$\text{Tsai}^{14} \quad u^+ = 12.7 \ln y^+ - 19.5 \quad (4b)$$

$$\text{Tomita}^{12} \quad u^+ = 10.0 \ln y^+ - 12.9 \quad (4c)$$

$$\text{Virk}^{11} \quad u^+ = 11.7 \ln y^+ - 17.0 \quad (4d)$$

$$\text{Huang}^{15} \quad u^+ = 13.0 \ln y^+ - 20.2 \quad (4e)$$

However, Van Driest⁴ postulates that the log-linear profile is not unique and that the coefficients are a function of polymer concentration.

The turbulent layer profile in both the above models is considered similar to the Newtonian turbulent layer but shifted upward in the law of the wall profile. The upward shift of the profile is dependent on the drag reduction. The mixing length constant has been found to be equal to that for Newtonian flows, indicating that polymer molecules do not affect the flowfield in this region. Though many researchers believe that drag reduction causes a thickened viscous sublayer, there is contradictory experimental evidence. The measurements of Tsai¹⁴ and Tomita¹² show an increase in the interactive layer thickness without a corresponding thickening of the sublayer, whereas Rudd's¹⁶ measurement with a laser anemometer shows a pronounced thickening of the sublayer.

A single-layer model which does not directly consider the polymer-flow interaction has been proposed by Poreh and Dimant,¹⁷ based on Van Driest's single-layer model for Newtonian flows. Huang¹⁵ extended the interactive layer model to include a fourth layer in which a velocity defect law is applicable. This four-layer model is the basis for the model presented in the following section.

Velocity Model in Developing Polymeric Field

With injection of concentrated polymer solution into a developing turbulent boundary-layer flow in the inlet region of a pipe, the polymer distribution across the boundary layer continuously changes from a highly nonuniform field near the injection point to a uniform field downstream. Since the polymer-flow interaction is confined to a wall layer, one can postulate that any nonuniform polymer distribution in this region would affect the interactive layer velocity profile without affecting the turbulent layer region profile.

Wang and Tullis¹⁸ have shown that a log-linear type velocity law accurately describes the flow in the entry region of a rough pipe over a large portion of the boundary layer for single-phase Newtonian flows. In the velocity model proposed for the nonhomogeneous polymer field in the inlet region, it is assumed that the similarity laws of Newtonian flow can be extended, as discussed by Huang.¹⁵ Based on experimental mean velocity profiles obtained at various x/D locations in the inlet region, the following mean velocity model is proposed:

1) Viscous sublayer

$$u^+ = y^+ \quad 0 \leq y^+ \leq y_p^+ \quad (5)$$

2) Polymer interactive layer

$$u^+ = (I/\kappa_p) \ln y^+ + B_p \quad y_p^+ \leq y^+ \leq y_\delta^+ \quad (6)$$

3) Turbulent layer

$$u^+ = (I/\kappa) \ln y^+ + B + \Delta B \quad y_\delta^+ \leq y^+ \leq \lambda(y/\delta) \quad (7)$$

4) Outer layer

$$U_c - u/u_* = - (I/\kappa) \ln (y/\delta) + (\pi/\kappa) \{ 1 + \cos [\pi(y/\delta)] \} \quad (y/\delta)_p \leq y/\delta < 1 \quad (8)$$

In this model the viscous sublayer is assumed to extend to $y^+ = 11.6$, as for Newtonian flow. Data for the polymer interactive layer in the developing polymeric region indicates that the velocity profile can be represented by a log-linear law. The slopes of the interactive layer profile defined by κ_p and the intercept B_p are not constant but are a function of both flow and polymer characteristics. The thickness of this layer y_p^+ is also a function of flow and polymer characteristics. In the turbulent layer, the velocity field is similar to the homogeneous polymeric flow, reflecting the fact that this inertially controlled layer is not affected by the polymer distribution. The magnitude of ΔB is a function of drag reduction. From turbulence measurements, Shieh² has shown that, with polymer injection, a strong intermittency occurs close to the injector. This implies that the region in which the turbulent profile is applicable should increase continuously with increasing x/D . The upper limit for the turbulent layer region varies from about 0.2 (y/δ) in the developing region to (y/δ) in the region of fully developed flow. The outer-layer defect profile is applicable in the region above the interactive layer. The overlap region with the turbulent layer increases as the boundary layer develops.

Velocity Model Coefficients

To define the previous mean velocity model, the parameters k , B , κ_p , B_p , ΔB , π and the dimensionless polymer interactive layer thickness y_p^+ must be evaluated. Wang and Tullis,¹⁸ using the same pipe as the present study, found a significant variation of κ and B occurred in the first 10 diam of the inlet region because of the nonlinear pressure gradient. Since the flow was in the transition regime, the magnitude of B was a function of Re . For this study, the value of κ is taken as 0.41 for $x/D > 7.5$. The intercept B was obtained from Ref. 18 for different Reynolds numbers and assumed constant for $x/D > 7.5$ for a given Reynolds number.

The drag reduction was found to be a rather complex function of C , τ_w , Re , and x/D . An analysis of the drag reduction data indicated that ΔB could be correlated to a drag reduction parameter $(V/u^*) (v_p/v_w)$ in which v_p is the viscosity of the polymer solution at the wall and v_w the viscosity of water.

Variation of ΔB with the drag reduction parameter is shown in Fig. 6. For this study, ΔB was obtained from velocity profile plots of u^+ vs y^+ . The parameter v_p/v_w was con-

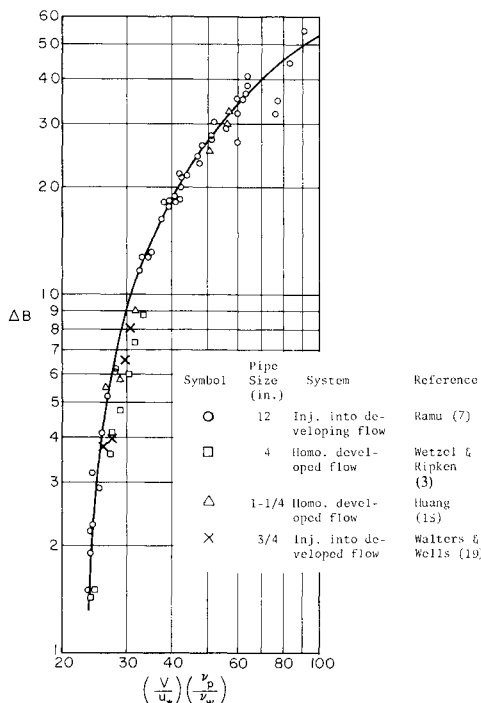


Fig. 6 Variation of ΔB with drag reduction parameter.

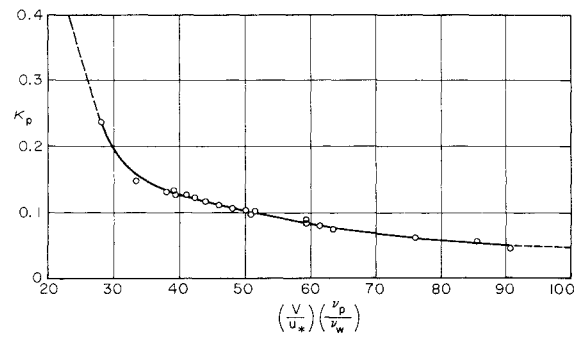


Fig. 7 Variation of κ_p with drag reduction parameter.

sidered to reflect the effect of polymer concentration at the wall, which varied from 1 to 1.45, corresponding to polymer wall concentrations from 1 to 300 ppm. Only the points above a parameter value of about 60 are for $v_p/v_w > 1.0$. Data from three other studies are also included. Wetzel and Ripken³ and Walters and Wells¹⁹ data, for which ΔB was measured from velocity plots, show a parallel shift. This could be due to differences in polymer batches or the result of system difference. The ΔB for Huang's¹⁵ data was computed from friction measurements.

In the polymer interactive layer the velocity profile coefficients were found to depend on both flow and polymer parameters. Though a log-linear type of profile fits the data in this region, the coefficients κ_p and B_p were not unique. The mixing length coefficient κ_p for the interactive layer was found to vary with the parameter $(V/u^*)(v_p/v_w)$, as shown in Fig. 7. The data were obtained from measured velocity profiles. For nondrag reducing flow $\kappa_p = \kappa$, as the profile in this region becomes part of the turbulent region. It is to be pointed out that, when κ_p is less than 0.086, the polymer interactive layer profile of this model would predict velocities less than the parabolic profile velocities in the lower portions of the polymer interactive layer.

The intercept B_p and the dimensionless polymer interactive layer thickness y_p^+ can be defined in terms of the other parameters. Equating Eq. (6) and the log-linear equation for Newtonian flow at the edge of the viscous sublayer

$$u/u^* = (1/\kappa) \ln 11.6 + B \quad (9)$$

yields

$$B_p = B - [(1/\kappa_p) - 1/\kappa] \ln 11.6 \quad (10)$$

further evaluation of Eqs. (6) and (7) with Eq. (10) at the edge of the polymer interactive layer yields a relationship between κ , κ_p , ΔB and y_p^+ as

$$\ln y_p^+ = \Delta B / [(1/\kappa_p) - 1/\kappa] + 2.45 \quad (11)$$

Thus, knowing κ_p and ΔB , one can evaluate y_p^+ and B_p .

The measured value of y_p^+ was found to vary with the wall concentration of polymer C_w , as shown in Fig. 8. The variation of y_p^+ with C_w can be expressed by the relationship

$$\ln y_p^+ = 6.28 - 2.52 [\ln (C_w/25)]^2 \quad (12)$$

The scatter in data is due to the fact that the velocity measurements in the polymer interactive layer at high wall concentration are affected by the viscoelastic property of the fluid and to the fact that a small variation in defining ΔB can vary y_p^+ over a wide range. It is interesting to note that the polymer interactive layer thickness is a maximum at a wall concentration of 25-30 ppm, which corresponds to the concentration for the maximum drag reduction that was obtained in the downstream fully mixed flow region. In the developing polymeric field, local drag reduction over 90% was obtained.

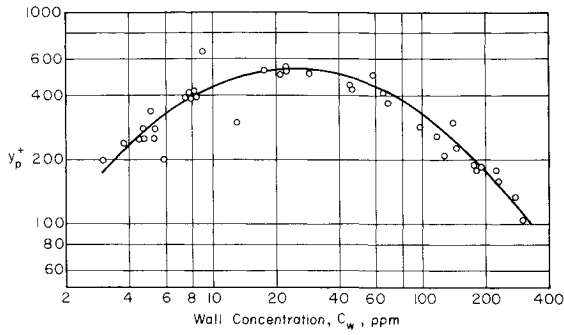
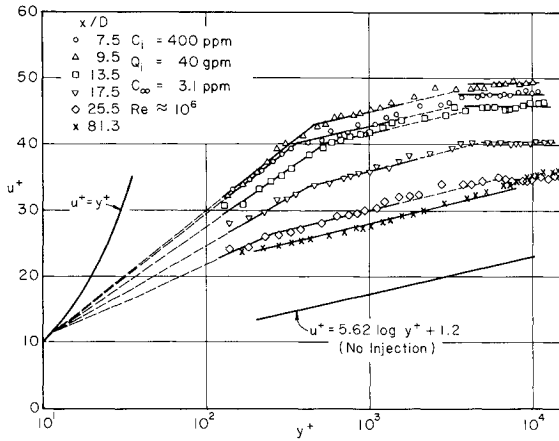
Fig. 8 Variation of y_p^+ with C_w .

Fig. 9 Velocity profiles at low injection rate.

At $X/D=13.5$ in the region of greatest drag reduction, the wall concentration was in excess of 175 ppm. The y_p^+ was about $\frac{1}{3}$ of the maximum value shown in Fig. 8. Thus, the concept of an increasing interactive layer thickness with drag reduction, as brought out in the interactive layer models, seems not to apply in a developing polymer field.

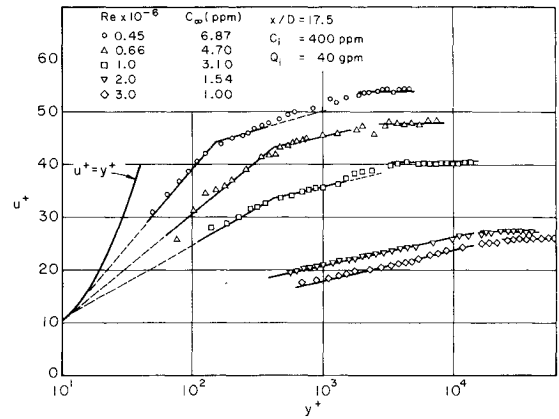
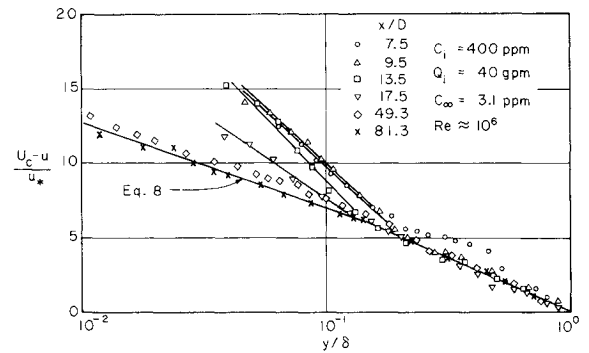
Velocity Profiles

Verification of the four-layer mean-velocity model came from velocity profile measurements taken at nine different locations in the inlet region. Most of the data used in confirming this model were for $C_i=400$ ppm, $Re=10^6$, and varying Q_i . At high injection rates some of the profiles in the interactive layer at locations close to the injector were influenced both by the injection disturbance and the high polymer concentration at the wall. Typical mean velocity profiles in the u^+-y^+ coordinate are shown in Figs. 9-11. Limitation of the pitot tube size prevented velocity measurements at y^+ values less than 70.

The wall shear stress τ_w and, hence, the shear velocity u^* in the inlet region were determined from pressure drop measurements discussed previously, using the relationship

$$f_p = 4(\tau_w / \frac{1}{2} \rho V^2) = 8(u^* / V)^2 \quad (13)$$

In the inlet region, where a nonlinear pressure gradient exists, τ_w can be obtained if the variation of momentum flux is known in addition to the pressure gradient. Poreh et al.⁸ have shown analytically that the contribution from the variation of momentum flux is small and that the pressure drop measurement can be used to estimate τ_w . This was also verified by Wang and Tullis¹⁸ for Newtonian flow. Shieh² estimated τ_w in the inlet region from hot film mean velocity data, assuming a log-linear relation for the velocity profile, and found that τ_w was within 5% of the values obtained from pressure drop measurements. The variation of momentum flux in this study was about 0.5% in the first 80 diameters.

Fig. 10 Velocity profiles at $x/D = 17.5$ for different Re .Fig. 11 Velocity profiles at $x/D = 17.5$ for different Re .

Based on these facts and the difficulty of measuring τ_w directly, it was felt that u^* obtained from Eq. (13) is appropriate.

The viscosity used in formulating y^+ was the viscosity of water ν_w . It is realized that, if one uses the polymer solution viscosity ν_p , the data will shift to lower y^+ values. The reasons: 1) since polymer distribution in the polymer developing region is nonuniform the value of ν_p will vary over the depth in a way still unknown, and 2) the polymer concentrations are so low that the change in viscosity normally is less than 3%.

Velocity profiles at various x/D 's for Re and C_i held constant for two different Q_i 's are shown in Figs. 9 and 10. The turbulent layer profile obtained for water flow in the rough pipe is also shown in these figures. The profiles at $x/D=7.5-25.5$ (Fig. 9) distinctly show the polymer interactive layer. Both the slope and the thickness continuously vary as the polymer layer develops and the wall concentration reduces. The thickness of the layer first increases as the wall concentration decreases, reaching a maximum thickness, and then decreases. The profiles beyond $x/D=25.5$ could not be extended into the interactive layer because of pitot tube size limitation. The maximum drag reduction for this Re at $x/D \approx 9.5$, as seen in Fig. 3, and this caused the maximum ΔB shift to occur at 9.5. Because of the higher wall concentration both the drag reduction and the ΔB shift were less at $X/D=7.5$. Beyond $x/D=9.5$, the reduction in wall concentration and the resulting decrease in drag reduction causes a continuous decrease in ΔB shift, as seen from profiles at 13.5, 17.5, and 25.5. Once the polymer concentration becomes uniform beyond $X/D=25.5$, both drag reduction and ΔB remain more or less unchanged. These profiles also indicate the presence of an outer flow, as evidenced by the deviation from turbulent layer profile. This region of outer flow begins at $y^+ \approx 1000$, corresponding to $y/\delta = 0.2$.

Velocity profiles at higher injection rates resulted in an increase in drag reduction ΔB shifts. Velocity data at $x/D=9.5$ and 13.5 showed scatter near the wall. Also, the high drag

reduction resulted in a reduced polymer interactive layer thickness. Therefore, one did not see the interactive layer profile at these locations. The profiles at $x/D=7.5, 9.5$, and 13.5 had u^+ values far in excess of the values given by any of the asymptotic profiles in Eq. (4). This fact was observed in other runs also. The polymer interactive layer profiles indicated that any single asymptote cannot define the profiles in this region, as has been suggested by the interactive layer models.

Effects of variation of Re on the mean velocity profile at $x/D=17.5$ are shown in Fig. 10. Re varies from 4.5×10^5 to 3×10^6 with $C_i=400$ ppm and $Q_i=40$ gpm. As would be expected, maximum drag reduction and ΔB shift decrease, due to decreasing C_∞ and degradation. The interactive layer thickness, which depends on the C_w , is seen to vary with Re. At $Re=2 \times 10^6$ and 3×10^6 , the drag reduction was not sufficient to overcome the negative roughness effect, with the result, that the interactive layer model fails to apply, even though the ΔB shift is in agreement with the proposed model.

The velocity defect profile (Fig. 11) fits the experimental data values of $\pi=0.30$ with $\kappa=0.41$. This value of π is the same as for water flow. The interactive layer profiles deviated from the defect profile law at y/δ values, depending on the polymer flows, is a function of the drag reduction parameter $(V/u^*)(v_p/v_w)$. In the inlet region, the limit of applicability of the turbulent layer profile increases from $y/\delta \approx 0.2$ at x/D flow direction. Beyond $y/\delta \approx 0.2$, the profiles followed Eq. (8) fairly well. The deviation of data at $x/D=7.5$ was partly due to disturbances of the injector.

Conclusions

1) Drag reduction in the inlet region varies with the amount of injected polymer, the wall shear stress (or Re), and distance from the injector. The drag reduction increases to a maximum, sometimes in excess of 90%, between 5 and 11 diam downstream from the injector, and then levels off to the homogeneous flow drag reduction value. The X/D at which drag reduction becomes constant is close to the location where the polymer concentration profile becomes uniform. This distance decreases as Re increases.

The total drag reduction in the inlet region integrated from $x/D=0$ to 81, at a given C_∞ and Re is independent of C_i , although the distribution of drag reduction near the injector varies with concentration. Drag reduction in the fully developed homogeneous region is a function of Re and concentration. A maximum drag reduction of 80% occurred at a concentration of 25 ppm. Degradation of polymer occurs for $Re \gtrsim 8 \times 10^5$. The degradation was more significant at low concentration.

The mean velocity profile in the developing region can be described by a layer-type model similar to that for homogeneous fully developed flow. However, the profile in the polymer interactive layer, the upward shift of the turbulent layer ΔB , and the profile parameter π are different.

The polymer interactive layer velocity profile is not universal but depends on the parameter $(V/u^*)(v_p/v_w)$. Velocity profiles at higher injection rates show that velocity in this region can exceed those given by any of the known asymptotic profiles of Eq. (4). The thickness of the polymer interactive layer y_p^+ in the developing polymer layer depends on the wall concentration.

The ΔB shift of the turbulent layer for developing and fully developed flows, as well as for homogeneous and developing polymer flows, is a function of the drag reduction parameter

$(V/u^*)(v_p/v_w)$. In the inlet region, the limit of applicability of the turbulent layer profile increases from $y/\delta \approx 0.2$ at $x/D=7.5$, to $y/\delta=1$ in the fully developed flow.

The outer flow region can be described by a velocity defect law of the type given in Eq. (8). Experimental results indicate a value of 0.3 for the profile parameter π for the inlet region flow.

References

- ¹Hoyt, J. W., "The Effect of Additives on Fluid Friction," *Journal of Basic Engineering, Transactions, ASME*, June 1972, pp. 258-285.
- ²Shieh, S.C., "Turbulence in Developing Boundary Layer with Polymer Additives," Ph.D. Thesis, Department of Civil Engineering, Colorado State University, Fort Collins, Colo., June 1974.
- ³Wetzel, J.H., Ripken, J.F., and Killen, J.M., "The Influence of Polymer Injection on a Large-Scale Boundary Layer," University of Minnesota, St. Anthony Falls Hydraulic Lab Memo. M-117, May 1969, Minneapolis, Minn.
- ⁴Van Driest, E.R., "Turbulent Drag Reduction of Polymer Solutions," *Journal of Hydraulics*, Vol. 4, July 1970, pp. 120-126.
- ⁵Merrill, E.W., Smith, K. A., Shin, H., and Mickley, H.S., "Study of Turbulent Flows of Dilute Polymer Solutions in a Couette Viscometer," *Transactions of the Society of Rheology*, Vol. 10, 1966, pp. 335-351.
- ⁶Tullis, J.P. and Ramu, K.L.V., "Drag Reduction in Developing Pipe Flow with Polymer Injection," *Proceedings for the International Conference on Drag Reduction*, British Hydraulics Research Association, Cambridge, England, Sept. 4-6, 1974, Paper G3, pp. G3-31 to G3-41.
- ⁷Tullis, J. Paul, and Ramu, K.L.V., "Viscous Drag Reduction in Developing Pipe Flow," Hydro Machinery Rept. 34, Colorado State University Engineering Research Center, prepared for the Naval Ship Research and Development Center, Nov. 1973, Fort Collins, Colo.
- ⁸Poreh, M., Rubin, H. and Elata, C., "Studies in Rheology and Hydrodynamics of Dilute Polymer Solution," Israel Institute of Techn. Haifa, Israel, Publ. 126, March 1969.
- ⁹Virk, P.S., "Drag Reduction in Rough Pipes," *Journal of Fluid Mechanics*, Vol. 45, P. 2, 1971, pp. 225-246.
- ¹⁰Meyer, W.A., "A Correlation of the Frictional Characteristics for Turbulent Flow of Dilute Viscoelastic Non-Newtonian Fluids in Pipes," *Journal of the American Institute of Chemical Engineers*, Vol. 12, May 1966, pp. 522-525.
- ¹¹Virk, P.S., "An Elastic Sublayer Model for Drag Reduction by Dilute Solutions of Linear Macromolecules," *Journal of Fluid Mechanics*, Vol. 45, P. 3, 1971, pp. 417-440.
- ¹²Tomita, Y., "Pipe Flows of Dilute Aqueous Polymer Solution," *Bulletin of the JSME*, Vol. 13, No. 61, July 1970, pp. 926-942.
- ¹³Giles, W.B., "Similarity Laws of Friction-Reduced Flows," *Journal of Hydraulics*, Vol. 2, Jan. 1968, pp. 34-40.
- ¹⁴Tsai, F.Y.E., "The Turbulent Boundary Layer in the Flow of Dilute Solutions of Linear Molecules," Ph.D. thesis, University of Minnesota, University Microfilms 69-11, 446, 1968, Minneapolis, Minn.
- ¹⁵Huang, T.T., "Similarity Laws for Turbulent Flow of Dilute Solutions of Drag-Reducing Polymers," Naval Ship Research and Development Center Rept. 4096, Aug. 1973, Bethesda, Md.
- ¹⁶Rudd, M.J., "Velocity Measurements Made with a Laser Dopplermeter on the Turbulent Pipe Flow of a Dilute Polymer Solution," *Journal of Fluid Mechanics*, Vol. 51, P. 4, 1972, p. 673-685.
- ¹⁷Poreh, M. and Dimant, Y., "Velocity Distribution and Friction Factors in Pipe Flows with Drag Reduction," Faculty of Civil Engrg., Technion, Israel Institute of Tech., Haifa, Israel, Publ. 175, Feb. 1972.
- ¹⁸Wang, J.S. and Tullis, J.P., "Turbulent Flow in the Entry Region of a Rough Pipe," *Journal of Fluids Engineering*, ASME, March 1974, pp. 62-68.
- ¹⁹Walters, R.R. and Wells, C.S., "Effects of Distributed Injection of Polymer Solutions on Turbulent Diffusion," *Journal of Hydraulics*, Vol. 6, July 1972, pp. 69-76.